



**HAL**  
open science

## Discerning different and opposite effects of hydrogenase on the corrosion of mild steel in the presence of phosphate species

Maha Mehanna, Ingrid Rouvre, Marie-Line Délia-Dupuy, Damien Féron,  
Alain Bergel, Régine Basséguy

### ► To cite this version:

Maha Mehanna, Ingrid Rouvre, Marie-Line Délia-Dupuy, Damien Féron, Alain Bergel, et al.. Discerning different and opposite effects of hydrogenase on the corrosion of mild steel in the presence of phosphate species. *Bioelectrochemistry*, 2016, 111, pp.31-40. 10.1016/j.bioelechem.2016.04.005 . hal-01907323

**HAL Id: hal-01907323**

**<https://hal.science/hal-01907323>**

Submitted on 29 Oct 2018

**HAL** is a multi-disciplinary open access archive for the deposit and dissemination of scientific research documents, whether they are published or not. The documents may come from teaching and research institutions in France or abroad, or from public or private research centers.

L'archive ouverte pluridisciplinaire **HAL**, est destinée au dépôt et à la diffusion de documents scientifiques de niveau recherche, publiés ou non, émanant des établissements d'enseignement et de recherche français ou étrangers, des laboratoires publics ou privés.



## Open Archive Toulouse Archive Ouverte (OATAO)

OATAO is an open access repository that collects the work of some Toulouse researchers and makes it freely available over the web where possible.

This is an author's version published in: <http://oatao.univ-toulouse.fr/20510>

**Official URL:** <https://doi.org/10.1016/j.bioelechem.2016.04.005>

### **To cite this version:**

Mehanna, Maha and Rouvre, Ingrid and Delia-Dupuy, Marie-Line and Féron, Damien and Bergel, Alain and Basséguy, Régine Discerning different and opposite effects of hydrogenase on the corrosion of mild steel in the presence of phosphate species. (2016) Bioelectrochemistry, 111. 31-40. ISSN 1567-5394

Any correspondance concerning this service should be sent to the repository administrator:  
[tech-oatao@listes-diff.inp-toulouse.fr](mailto:tech-oatao@listes-diff.inp-toulouse.fr)

# Discerning different and opposite effects of hydrogenase on the corrosion of mild steel in the presence of phosphate species

Maha Mehanna<sup>a</sup>, Ingrid Rouvre<sup>a</sup>, Marie-Line Delia<sup>a</sup>, Damien Feron<sup>b</sup>, Alain Bergel<sup>a</sup>, Régine Basseguy<sup>a,\*</sup>

<sup>a</sup> Laboratoire de Génie Chimique, Université de Toulouse, CNRS, INPT, UPS, Toulouse, France

<sup>b</sup> Den-SERVICE de la Corrosion et du Comportement des Matériaux dans leur Environnement (SCCME), CEA, Université Paris-Saclay, F-91191 Gif-sur-Yvette, France

## A B S T R A C T

Mild steel coupons were exposed to hydrogenase in a 10 mM phosphate solution. Control coupons were covered by a layer of vivianite. The injection of hydrogenase caused a fast increase in the open circuit potential; this increase depended on the amount of hydrogenase injected and increased from 8 mV for 30  $\mu$ L hydrogenase to 63 mV for 80  $\mu$ L. The presence of enzyme resulted in a thicker deposit: high amounts induced the accumulation of corrosion products. Hydrogenase that was deactivated by air revealed a protective effect: non-degradation was observed. In contrast, hydrogenase that was denatured by heat provoked an important deposit of corrosion products with a heterogeneous, cracked structure. The study showed that the action of hydrogenase is not linked to its regular enzymatic activity but to a balance between the protective effect of its protein shell and the electrochemical action of its iron-sulphur clusters. Depending on the operating conditions, hydrogenase can either enhance or mitigate the formation of a corrosion layer on mild steel.

## Keywords:

Hydrogenase  
Mild steel  
Phosphate medium  
Microbial corrosion  
Microbially influenced corrosion

## 1. Introduction

Sulphate-reducing bacteria and thiosulphate-reducing bacteria (SRB/TRB) are the most clearly identified causes of anaerobic microbially influenced corrosion (MIC) of steels in natural environments [1–7]. Several mechanisms have been proposed to explain anaerobic MIC by SRB and TRB [8–15]. As far as SRB are concerned, the most often evoked mechanism is based on the production of sulphide ions by the metabolic reduction of sulphates. Sulphide ions react with iron ions, forming iron sulphide which deposits on the material surface and catalyses the reduction of proton:



Several studies have discussed the efficiency of iron sulphides in catalysing proton reduction depending on the crystal state and the structure of the deposit [16–17]. Contrarily to what has been said sometimes in the past, the consumption of the final hydrogen, by SRB or other means, cannot have a direct effect on the corrosion rate [18]. In Eq. (1) the forward reaction of electron uptake by the proton is the rate-limiting step on steel surfaces in anaerobic environments. Consuming the final hydrogen product cannot consequently have any direct effect on the rate of electron extraction from the material. Consequently, consuming the final hydrogen cannot enhance the corrosion process. Consumption of hydrogen by SRB can only have an indirect effect

by promoting the development of SRB on the material surface and enhancing the production of sulphide ions, for instance.

Some studies have demonstrated that there is a direct correlation between the presence of hydrogenase in SRB and corrosion [19–20], while it has also been claimed that a hydrogenase-negative strain of SRB is more corrosive than hydrogenase-positive strains [21]. Hydrogenases are a group of enzymes that catalyse the reversible oxidation of hydrogen (Eq. (1)) [22–23]. Hydrogenases are divided into three groups according to the composition of their active site [22,24]: [NiFe]-, [FeFe]-, and the Fe—S cluster-free hydrogenases (initially called metal-free and now renamed [Fe]-hydrogenase [25–26]). The [NiFe]- and [FeFe]-enzymes form the vast majority. [FeFe]-hydrogenases are known to have 100 times more H<sub>2</sub> production specific activity than [NiFe]-hydrogenases [27]. In the metabolic pathway, they transfer the electrons to specific redox partners (Med) like cytochromes, nicotinamide adenine dinucleotide (NAD<sup>+</sup>) or ferredoxin (Fd<sub>ox</sub>). They also can use artificial mediators as electron acceptors. For instance, the [Fe]-hydrogenase from *Clostridium acetobutylicum* that was used in this work can exchange electrons with ferredoxin (natural partner) or methyl viologen (artificial mediator), both following the global reaction:



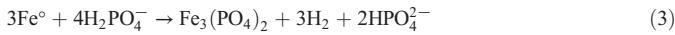
Hydrogenases have been claimed to be involved in corrosion mechanisms either by being present inside bacterial cells or by being free after cell lysis [20,28]. Several studies have tried to elucidate the possible effect of free hydrogenases on the corrosion of steels and have proposed two kinds of mechanisms.

\* Corresponding author.

E-mail address: regine.basseguy@ensiacet.fr (R. Basseguy).

### 1.1. Mechanism 1: catalysis of hydrogen consumption with involvement of phosphate species (Schematic 1)

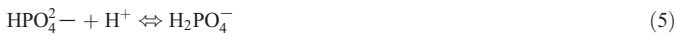
A synergetic effect of hydrogenase and phosphate species on corrosion was first pointed out by Bryant and Laishley [29–30], who observed that hydrogenase increased the corrosion rate of carbon steel when used in a phosphate solution. These authors proposed a direct reaction between steel and phosphate ions:



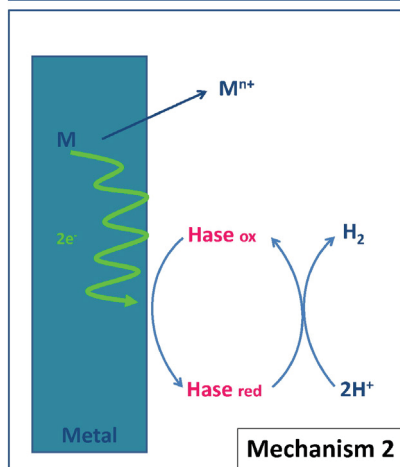
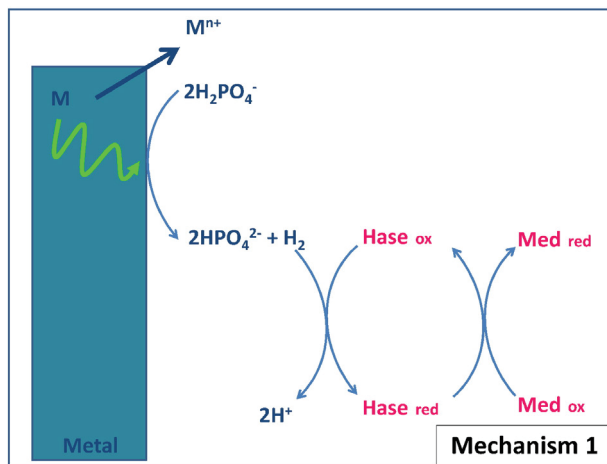
This mechanism was then reworked, demonstrating that phosphate species undergo a so-called cathodic deprotonation on steel surfaces [31]:



This reaction, coupled with acid equilibrium:



presents the phosphate species as an efficient homogeneous catalyst for the reduction of proton/water [8]. The cathodic deprotonation of phosphate species (Reaction (4)) is relatively fast on steel surfaces



**Scheme 1.** Mechanisms for hydrogenase action on steel corrosion in anaerobic phosphate medium; a) Mechanism 1: Catalysis of hydrogen consumption with involvement of phosphate species. b) Mechanism 2: catalysis of proton reduction by adsorbed hydrogenase. Hase is for hydrogenase in its reduced (red) or oxidized (Ox) form. Med is for mediator in its reduced (red) or oxidized (Ox) form.

and not strictly limited by the forward electron uptake (as is Eq. (1)). On steel surfaces, Reaction (4) is a balanced reaction that can be shifted by the consumption of hydrogen. In this case, with significant concentrations of phosphate in the solution, the consumption of hydrogen can increase the rate of electron extraction from the material, and consequently increase corrosion. This process has been shown on mild steel using hydrogenase from *Ralstonia eutropha*, which catalysed the oxidation of hydrogen with  $\text{NAD}^+$  as a final electron acceptor [32]. However hydrogenase can enhance corrosion following this mechanism only in the presence of two different compounds:

- a compound able to ensure a balanced cathodic deprotonation (like phosphate species, Reaction (4))
- a final electron acceptor, with which the enzyme is able to work (depends on the hydrogenase species).

### 1.2. Mechanism 2: catalysis of proton reduction by adsorbed hydrogenase (Schematic 1)

The second mechanism is based on the direct catalysis of proton reduction by adsorbed hydrogenase. The catalysis by adsorbed hydrogenase of direct electron extraction from different metals has already been demonstrated in the literature. Hydrogenases from *Thiocapsa roseopersicina* and *Lamrobacter modestohalophilus* have been shown to catalyse the oxidation of metals directly, without the need for a mediator [33]. Hydrogenases from *T. roseopersicina* and *Alcaligenes eutrophus* can use cadmium particles directly as electron donors to produce hydrogen or to reduce  $\text{NAD}^+$ . It has been assumed that this mechanism can accelerate metal dissolution and thus be a key to MIC processes [34]. Moreover, hydrogenases from *Methanococcus maripaludis* can use iron granules to produce hydrogen by a direct electron transfer [35]. As well, on pyrolytic graphite, hydrogenases from *Escherichia coli* are able to catalyse some electrochemical reactions which are only possible with a large overpotential in absence of catalyser [36]. Hydrogenase from *R. eutropha* (new name for *A. eutrophus*) adsorbed on stainless steel has also been claimed to create a direct cathodic reaction on stainless steel [37]. Nevertheless, in this case, because of the presence of both a final electron acceptor and phosphate buffer, significant involvement of Mechanism 1 may be suspected.

Catalysis of electron extraction by adsorbed hydrogenase has been evoked several times in the literature as a likely key step in anaerobic MIC. Nevertheless, to our knowledge, our previous work carried out with hydrogenase from *C. acetobutylicum* was the first experimental demonstration that hydrogenase increased the corrosion of steel [38]. In this study, experiments have been performed in the absence of any final electron acceptor other than protons and water. In this condition, hydrogenase cannot oxidise the hydrogen that results from the corrosion process. Consequently Mechanism 1 cannot occur and hydrogenase can act only via the direct catalysis of proton or water reduction.

The purpose of the current study was to progress in deciphering the fine mechanisms of hydrogenase action in the corrosion of mild steel. The high concentration of phosphate that was used in the previous study (100 mM) interfered with the results because of the large amount of vivianite that formed rapidly on the steel surface. Here, the experiments were performed with less concentrated phosphate solutions (10 mM). No other electron acceptor than proton and water was present in solution, neither natural redox partner (oxidised ferredoxin) nor artificial mediator, in order to avoid the occurrence of Mechanism 1.

## 2. Materials and methods

### 2.1. Chemicals and biochemicals

Solutions were prepared in deionised water (ELGA PURELAB, 10–15  $\text{M}\Omega \cdot \text{cm}$ ) with analytical grade chemicals: sodium dihydrogenophosphate (Prolabo), tris(hydroxyl-methyl) aminomethane (named

Tris-HCl from Acros Organic), hydrochloric acid (Acros Organics), and sodium hydroxide. *C. acetobutylicum* cells were cultured and hydrogenase extracted following the procedures reported elsewhere [39]. Hydrogenase solution was divided into aliquots that were stored at  $-80\text{ }^{\circ}\text{C}$ . Each aliquot was used only once in order to limit loss of activity. For a given set of experiments, all the aliquots came from the same purification process. Hydrogenase activity was measured at  $37\text{ }^{\circ}\text{C}$  for  $\text{H}_2$  consumption in a phosphate buffer  $0.1\text{ M}$  pH 7.2. The purified hydrogenase used in the study, had a specific activity of  $194,339\text{ }\mu\text{mol min}^{-1}\text{ mg}^{-1}$  that led to an activity of  $4250\text{ }\mu\text{mol min}^{-1}\text{ mL}^{-1}$  (or  $4250\text{ Units}\cdot\text{mL}^{-1}$ ) in the aliquots. Injecting  $30\text{ }\mu\text{L}$ ,  $50\text{ }\mu\text{L}$  or  $80\text{ }\mu\text{L}$  hydrogenase into the  $50\text{ mL}$  cells was equivalent to final activities of around  $2.5\text{ U}\cdot\text{mL}^{-1}$ ,  $4.25\text{ U}\cdot\text{mL}^{-1}$  and  $6.8\text{ U}\cdot\text{mL}^{-1}$  respectively.

## 2.2. Electrochemical measurements

The electrochemical experiments were performed with a three-electrode system in closed cells (Metrohm) containing  $50\text{ mL}$  solution. The working electrodes were  $2\text{-cm-diameter}$  cylinders of 1145 mild steel purchased from Thyssen Krupp Materials, France (elemental composition by weight percentage:  $0.46\text{ C}$ ,  $0.31\text{ Si}$ ,  $0.65\text{ Mn}$ ,  $0.01\text{ P}$ ,  $0.032\text{ S}$ ,  $0.1\text{ Cr}$ ,  $0.1\text{ Ni}$ ,  $0.02\text{ Mo}$ ,  $0.05\text{ Al}$ ,  $0.11\text{ Cu}$ ) embedded in resin (Resipoly Chrysor). The electrical connection was made through titanium wire screwed into the steel sample and protected with resin. Coupons were ground successively with SiC papers of P120, P180, P400, P800, P1200, P2400, P4000 grit (Lam Plan) and rinsed thoroughly with distilled water. A platinum-iridium ( $10\%$  iridium) grid was used as the auxiliary electrode and a saturated calomel electrode (SCE, radiometer analytical) as the reference.

The electrochemical cell was hermetically closed. The steel coupon was first maintained above the solution surface while nitrogen was continuously bubbled into the solution for  $40\text{ min}$ . It was then immersed into the solution and the nitrogen flow was maintained during the whole experiment.  $15\text{ min}$  after the coupon was immersed in the solution, hydrogenase was injected with a syringe in strict anaerobic conditions, oxygen having been removed from the syringe with nitrogen. All experiments were carried out at room temperature.

The electrochemical measurements were performed by using a VMP2 multipotentiostat (Bio-Logic, SA) monitored by the software EC-lab 9.2. The open-circuit potential ( $E_{oc}$ ), also called free corrosion potential, was monitored over time when the steel coupon was immersed in the solution for  $24\text{ h}$ . Polarisation resistance ( $R_p$ ) was recorded every  $4\text{ h}$  using voltammetry technique around the  $E_{oc}$  scanning the potential from  $E_{oc} - 10\text{ mV}$  to  $E_{oc} + 10\text{ mV}$ , at  $0.2\text{ mV s}^{-1}$ .

Considering the Tafel law for the anodic (mainly oxidation of iron) and cathodic (mainly reduction of proton/water) reactions, the anodic ( $i_a$ ) and cathodic ( $i_c$ ) currents are given by Eqs. (6) and (7):

$$i_a = i_{corr} \left\{ \exp \left[ \frac{\alpha_a F}{RT} (E - E_{corr}) \right] \right\} \quad (6)$$

$$i_c = i_{corr} \left\{ - \exp \left[ \frac{-\alpha_c F}{RT} (E - E_{corr}) \right] \right\} \quad (7)$$

where  $\alpha_a$  and  $\alpha_c$  are the anodic and cathodic transfer coefficients, respectively,  $i_{corr}$  is the corrosion current density and  $E_{corr}$  the corrosion potential [40].

In the vicinity of  $E_{corr}$ , the global current ( $i_a + i_c$ ) can be linearized using the Stern-Geary model [41] that results in the following:

$$i_a = i_c = i_{corr} \left[ \left[ 1 + \frac{\alpha_a F}{RT} (E - E_{corr}) \right] - \left[ 1 - \frac{\alpha_c F}{RT} (E - E_{corr}) \right] \right] \quad (8)$$

$$i_a + i_c = i_{corr} (E - E_{corr}) (1/\beta_a + 1/\beta_c). \quad (9)$$

Eq. (9) is the equation of a straight line. Consequently, the slope of the polarisation curve in the vicinity of the corrosion potential ( $\Delta i/\Delta E$ ) is proportional to the corrosion rate (which is proportional to the corrosion current density) and corresponds to the inverse of the polarisation resistance ( $R_p$ ) as follows:

$$\Delta i/\Delta E = i_{corr}/B = R_p^{-1} \quad (10)$$

with

$$B = (\beta_a \beta_c) / (\beta_a \beta_c). \quad (11)$$

Software based on this Stern-Geary model was used to determine the polarisation resistances  $R_p$  from the experimental current-potential measurements.

## 2.3. Surface imaging and analysis

Metal deterioration was assessed by Scanning Electron Microscopy (SEM) using a LEO 435 VP-Carl Zeiss SMT ( $10,000\times$  magnification,  $10\text{ kV}$  acceleration voltage). Surface chemical analysis was performed by energy dispersive X-ray analysis (EDX). For each sample, the average values and standard deviations resulted from many measurements performed at different spots on the sample surface.

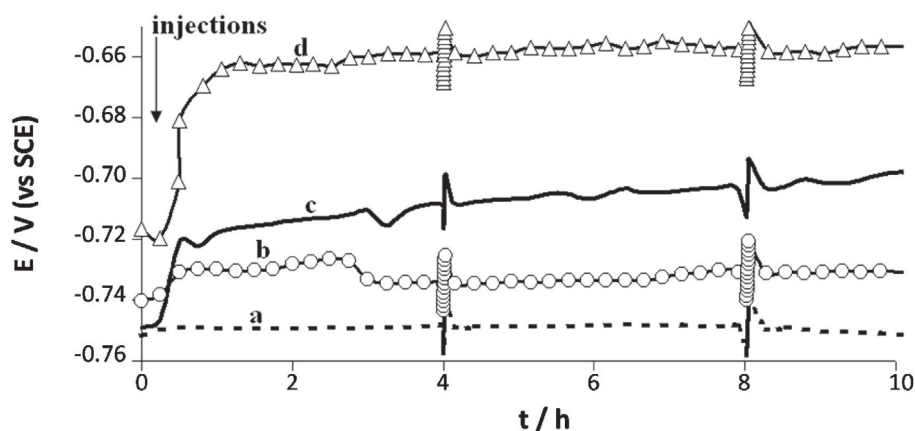


**Fig. 1.** Open circuit potential versus time for 1145 carbon steel electrode immersed in anaerobic  $10\text{ mM}$  phosphate solution pH 7.2, with or without addition of hydrogenase. Fluctuations of  $\pm 10\text{ mV}$  that appeared on the graph every four hours were due to polarization resistance measurements a)  $\text{---}$  without injection; b)  $\text{---}\circ\text{---}$  with  $30\text{ }\mu\text{L}$  hydrogenase; c)  $\text{---}$  with  $50\text{ }\mu\text{L}$  hydrogenase; d)  $\text{---}\triangle\text{---}$  with  $80\text{ }\mu\text{L}$  hydrogenase.

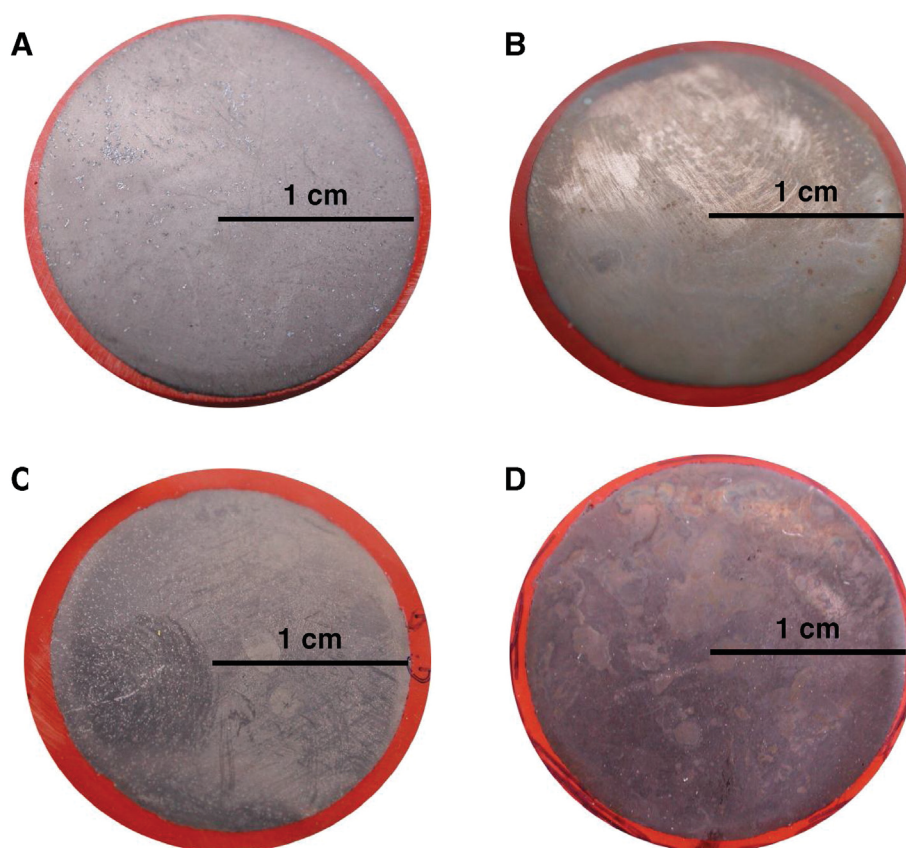


**Fig. 2.** Photographs of 1145 carbon steel coupons after 24 hour immersion in anaerobic 10 mM phosphate solution pH 7.2 in the absence of hydrogenase (A) and in the presence of 30  $\mu$ L hydrogenase (B), 50  $\mu$ L hydrogenase (C) and 80  $\mu$ L hydrogenase (D).

### 3. Results and discussion

#### 3.1. Influence of active hydrogenase on open circuit potential and deposit composition

Mild steel 1145 coupons were immersed in phosphate solution 10 mM, pH 7.2 for 24 h. The electrochemical cell was hermetically closed and great care was taken to bring the steel coupon into contact with the solution only after it had been strictly deoxygenated (see the [Materials and methods](#) section). The potential was stabilised for 15 min and hydrogenase was then injected in strictly anaerobic

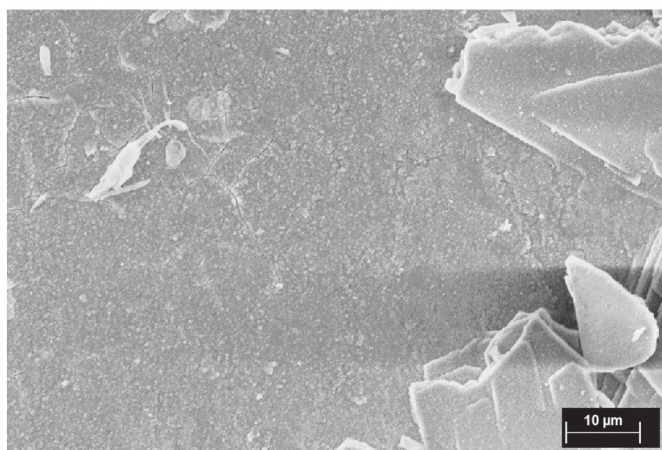


**Fig. 3.** SEM micrograph for 1145 carbon steel surface after 24 hour immersion in anaerobic 10 mM phosphate solution pH 7.2, in the absence of hydrogenase. 10000  $\times$  magnification, 10 kV acceleration voltage.

conditions, because the hydrogenase from *C. acetobutylicum* is highly sensitive to oxygen. The variation of the open-circuit potential  $E_{oc}$  was recorded as a function of time for 24 h (Fig. 1).

Seven control experiments were performed without any injection, or with injection of only deoxygenated phosphate solution at  $t = 15$  min, to check that the injection process did not introduce traces of oxygen into the cell. No significant potential evolution was observed. After 24 h immersion, the electrode was covered by a uniform, greyish film (Fig. 2A) that tended to become bluish on exposure to air, a behaviour that is characteristic of vivianite ( $Fe_3(PO_4)_2 \cdot 8H_2O$ ) [42]. SEM micrography of these coupons (immersed in the absence of hydrogenase) showed a grey surface with the presence of crystals (Fig. 3). EDX analyses averaged over different spots of the surface did not reveal the presence of carbon although it was clearly detected on clean coupons before they were immersed in the phosphate solution, confirming that the deposit coated uniformly the surface of the coupon. In terms of atomic mass percentages, the deposit was mainly composed of iron (51–64%) and oxygen (32–38%) (Table 1). The percentage of phosphorous, around 3%, was smaller than expected for pure vivianite, which usually contains around 9% phosphorous. As the amounts of iron were rather high, the deposit was probably a mixture of vivianite and iron oxide. Moreover, other products containing simultaneous iron and phosphorous were also suggested in literature: for instance, the formation of an amorphous type of iron phosphide  $Fe_2P$  is possible, this deposit was observed under biotic and abiotic conditions, especially when culture media for testing microbial corrosion are supplemented with phosphates and sulphates [43,44]. A compound with average stoichiometric formula  $Zn_{0.5}K_{1.1}PO_{3.35}Fe_{0.4}$  was also detected during the protection process of 1138 carbon steel by zinc phosphatation followed by a post-treatment with potassium monofluorophosphate [45].

As shown in Fig. 1, injecting hydrogenase caused a fast increase in potential. Most of the potential increase occurred during the first hour

**Table 1**

EDX analysis (atomic mass %) of 1145 carbon steel surface after 24 h immersion in anaerobic 10 mM phosphate solution pH 7.2, with or without hydrogenase.

Hydrogenase amount/ element	Fe	O	P	C	K	Cl	Mn	Na
Control, no hydrogenase 0 $\mu\text{L}^{\text{a}}$	64/51	32/38	3/4	—	0/1	1/2	—	—
80 $\mu\text{L}$ hydrogenase <sup>b</sup>	61 $\pm$ 16	16 $\pm$ 10	—	22 $\pm$ 21	—	1 $\pm$ 0.9	—	—
30 $\mu\text{L}$ heated hydrogenase On deposit (spot 1 in Fig. 7C)	45	40	6	—	0.5	—	0.5	8
30 $\mu\text{L}$ heated hydrogenase In crack (spot 2 in Fig. 7C)	83	14	—	—	—	—	—	2

<sup>a</sup> Maximum/minimum values.<sup>b</sup> Mean and standard deviation for 5 points analysed.**Table 2**Potential ennoblement  $\Delta E$  ( $E_t = 7.5 \text{ h} - E_t = 15 \text{ min}$ ) and visual aspect of the surface at the end of the experiments ( $t = 24 \text{ h}$ ) for 1145 carbon steel coupons immersed in anaerobic 10 mM phosphate solution pH 7.2, with or without hydrogenase.

Hydrogenase amount/corresponding activity	$\Delta E$ (mV)	Visual aspect of the surface
0 $\mu\text{L}/0 \text{ U} \cdot \text{mL}^{-1}$	1	Uniform deposit containing vivianite
30 $\mu\text{L}/2.5 \text{ U} \cdot \text{mL}^{-1}$	8	Deposit containing vivianite and a few pits
50 $\mu\text{L}/4.25 \text{ U} \cdot \text{mL}^{-1}$	48	Thick greyish deposit
80 $\mu\text{L}/6.8 \text{ U} \cdot \text{mL}^{-1}$	63	Marked heterogeneous red deposit
30 $\mu\text{L}$ -oxygenated/ $0 \text{ U} \cdot \text{mL}^{-1}$	7	No visible deposit
30 $\mu\text{L}$ -heated/ $0 \text{ U} \cdot \text{mL}^{-1}$	26	Thick deposit containing vivianite with deep cracks

after injection of the enzyme. Full potential increase values ( $\Delta E$ ) were evaluated by subtracting the value of the potential just before hydrogenase injection ( $t = 15 \text{ min}$ ) from the value at  $t = 7.50 \text{ h}$  (before the second polarisation resistance measurement).  $\Delta E$  depended on the amount of hydrogenase injected and increased from 8 mV for 30  $\mu\text{L}$  hydrogenase to 63 mV for 80  $\mu\text{L}$  (Table 2). The visual aspects of the deposits obtained after 24 h were also clearly dependent on the amount of hydrogenase (Table 2). With 30  $\mu\text{L}$  hydrogenase, the coupon was covered with a bluish mineral that indicated a marked presence of vivianite ( $\text{Fe}_3(\text{PO}_4)_2 \cdot 8\text{H}_2\text{O}$ ). A few pits that turned red when exposed to air also indicated the presence of slight local corrosion (Fig. 2B). Addition of 50  $\mu\text{L}$  hydrogenase increased the free potential up to 43 mV and the electrode was covered by a grey deposit that seemed more thick (Fig. 2C). 80  $\mu\text{L}$  hydrogenase led to a green deposit that was unstable and turned red in contact with air, corresponding to a large production of iron hydroxides  $\text{Fe}(\text{OH})_2$  and  $\text{Fe}(\text{OH})_3$  (Fig. 2D) [46]. SEM surface analysis of coupons exposed to 80  $\mu\text{L}$  hydrogenase (coupon D) showed a highly heterogeneous corrosion layer: some surface zones were covered by small crystals (Fig. 4A) and an heterogeneous deposit appeared on others (Fig. 4B). The chemical analysis of the corrosion products on the surface gave

around 61% iron, 22% carbon and 16% oxygen (Table 1). The high percentages of iron and carbon indicated that the steel surface was certainly reached by the EDX probe in the zones where the deposit was not present. The standard deviations of the measurements made on 5 different spots, which were significantly higher than for the previous measurements (Table 1), confirmed that the deposit had an heterogeneous chemical composition. In contrast with all the other cases, no phosphorous was detected in the presence of 80  $\mu\text{L}$  hydrogenase. This is in agreement with the visual observation of the electrode (Fig. 2D), where the surface of the steel was covered by a reddish iron oxide layer and no vivianite was detected. It can be concluded that a large amount of hydrogenase accelerated the formation of the corrosion products with a FeII/FeIII ratio unfavorable to vivianite deposition.

### 3.2. Effect of deactivated and denatured hydrogenase

Similar experiments were performed with hydrogenase that was previously deactivated by exposure to air for 2 h and 30 min or denatured by heating the aliquot at 100 °C for 30 min until the solution boiled (Fig. 5).

Injection of 30  $\mu\text{L}$  hydrogenase aliquot deactivated by exposure to air increased the free potential by 7 mV. At the end of the experiment, no deposit was visible on the surface of the electrode. On the contrary, the electrode was still electrically conductive and reflected the light as shown in Fig. 6 where the image of the camera lens can be seen on the coupon surface.

Addition of 30  $\mu\text{L}$  hydrogenase denatured by heating increased the free potential by 26 mV. At the end of the experiment, the mild steel electrode surface was covered by an important non-conductive deposit with cracks spreading all over the layer (Fig. 7).

The surface was analysed carefully discriminating two different zones: on the upper side of the deposit (Fig. 7C spot 1) and in the crack (Fig. 7C spot 2). EDX analysis (Table 1) indicated that the amount of iron on the top of the layer (45%) was around half that in the crack (83%). Phosphorous was present in the deposit (6%) whereas it was not detected in the

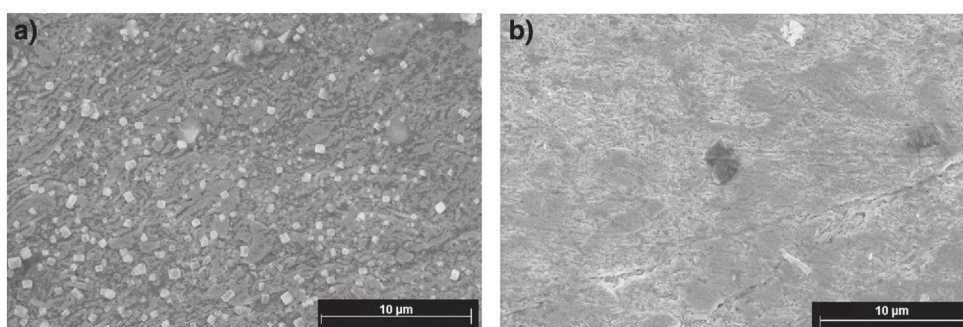


**Fig. 4.** SEM micrographs of 1145 carbon steel surface after 24 hour immersion in anaerobic 10 mM phosphate solution pH 7.2, containing 80  $\mu\text{L}$  hydrogenase: a zone covered by small crystals (A) and a zone with a heterogeneous deposit (B). 10000  $\times$  magnification, 10 kV acceleration voltage.

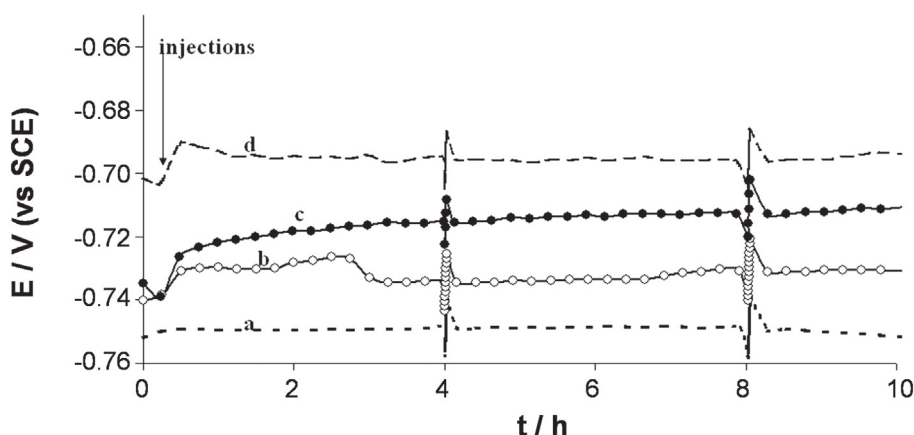


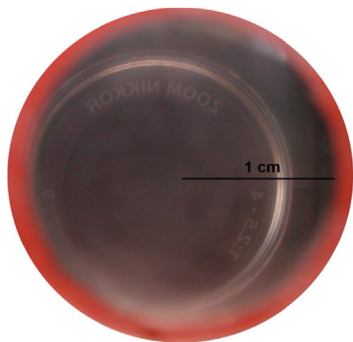
**Fig. 5.** Variation of the open circuit potential versus time for 1145 carbon steel coupons immersed in anaerobic 10 mM phosphate solution pH 7.2, with hydrogenase (in different states) or without hydrogenase. Fluctuations of  $\pm 10$  mV that appear every four hours were due to polarisation resistance measurements. a)  $\text{---}$  without injection; b)  $\text{---}\circ\text{---}$  with 30  $\mu\text{L}$  hydrogenase; c)  $\text{---}\bullet\text{---}$  with 30  $\mu\text{L}$  heated hydrogenase; d)  $\text{---}\text{---}$  with 30  $\mu\text{L}$  oxygenated hydrogenase.

crack. These data indicate that the deposit was made up of corrosion products mixed with vivianite, while only iron and iron hydroxides/oxides were present inside the cracks. The cracks were anodic areas where corrosion was occurring, while the phosphate layer was protective.

### 3.3. Measures of $R_p$ and estimation of corrosion rate

During the immersion, a potential scan was performed every 4 h, at  $0.2 \text{ mV s}^{-1}$  around the open circuit potential ( $E_{oc}$ ) in the range

a)



b)



**Fig. 6.** Photograph (A) and SEM micrograph (B) of 1145 carbon steel surface after 24 hour immersion in anaerobic 10 mM phosphate solution pH 7.2 in the presence of 30  $\mu\text{L}$  hydrogenase deactivated by air. SEM characteristics: 10000  $\times$  magnification, 10 kV acceleration voltage.

[ $E_{oc} - 10 \text{ mV}$ ,  $E_{oc} + 10 \text{ mV}$ ]. The Stern-Geary model was used to determine the polarisation resistances  $R_p$  from the experimental current-potential measurements (Fig. 8). The values of  $1/R_p$  that give an evaluation of the corrosion rates (Eq. (10)) are gathered in Table 3.

Seven control experiments performed without hydrogenase showed identical  $1/R_p$  that means identical  $i_{corr}$  values, which remained stable during the 24 h experiments. In particular, only a slight modification of  $1/R_p$  values was observed during the first 2 h of immersion from  $8$  to  $9.10^{-4} \Omega^{-1} \cdot \text{cm}^{-2}$ , then it did no longer significantly vary. A  $1/R_p$  value around  $6.10^{-4} \Omega^{-1} \cdot \text{cm}^{-2}$  (average value from seven experiments) can be considered as the stable estimated corrosion current that corresponds to the “mild steel/10 mM phosphate solution” interface used here. It can be noticed that these values were close to those reported in the literature for mild steel at open circuit conditions [47]. Indeed, in  $\text{NaH}_2\text{PO}_4$  0.1 M, pH 6.0,  $R_p$  has been noted to increase from  $188 \Omega \cdot \text{cm}^2$  (i.e.  $1/R_p = 5.3.10^{-3} \Omega^{-1} \cdot \text{cm}^{-2}$ ) at 1 min to  $1516 \Omega \cdot \text{cm}^2$  (i.e.  $1/R_p = 6.7.10^{-4} \Omega^{-1} \cdot \text{cm}^{-2}$ ) at 60 min.

For the experiments performed with hydrogenase, Tafel plots were recorded every 4 h. No measurement was made in the period  $t = 0$  to  $t = 4$  h to avoid any possible disturbance for the surface state of the coupons. In the presence of the hydrogenase,  $1/R_p$  values remained almost constant in all cases and lower than the  $6.10^{-4} \Omega^{-1} \cdot \text{cm}^{-2}$  obtained in control experiments, except for the heated hydrogenase. In agreement with the variation of the free potential,  $1/R_p$  values indicated that the main action of hydrogenase occurred before 4 h. After 4 h,  $1/R_p$  values indicate a “passive” behaviour of the mild steel due to the phosphate treatment and the vivianite formation, which was favoured by the presence of hydrogenase. This favourable effect of hydrogenase on the formation of a protective deposit of vivianite has already been shown [32]. The heated hydrogenase induced more complex behaviour, with a first increase of  $i_{corr}$  (high values of  $1/R_p$ ) followed by a slow continuous decrease. Heated hydrogenase increased corrosion rate and then the formation of a thick deposit slowed down corrosion. The presence of cracks where corrosion could continue explained why  $1/R_p$  (thus  $i_{corr}$ ) remained higher for some hours with respect to the other cases that did not show deep cracks.

### 3.4. Discussion of the mechanisms

In the control experiments no local corrosion was observed after 24 h,  $i_{corr}$  was almost constant ( $1/R_p$  around  $6.10^{-4} \Omega^{-1} \cdot \text{cm}^{-2}$ ) and coupons were covered with a layer containing vivianite, which is known to have a protective effect. Vivianite is an iron (II) phosphate, which may be used as a corrosion inhibiting layer on steel surfaces

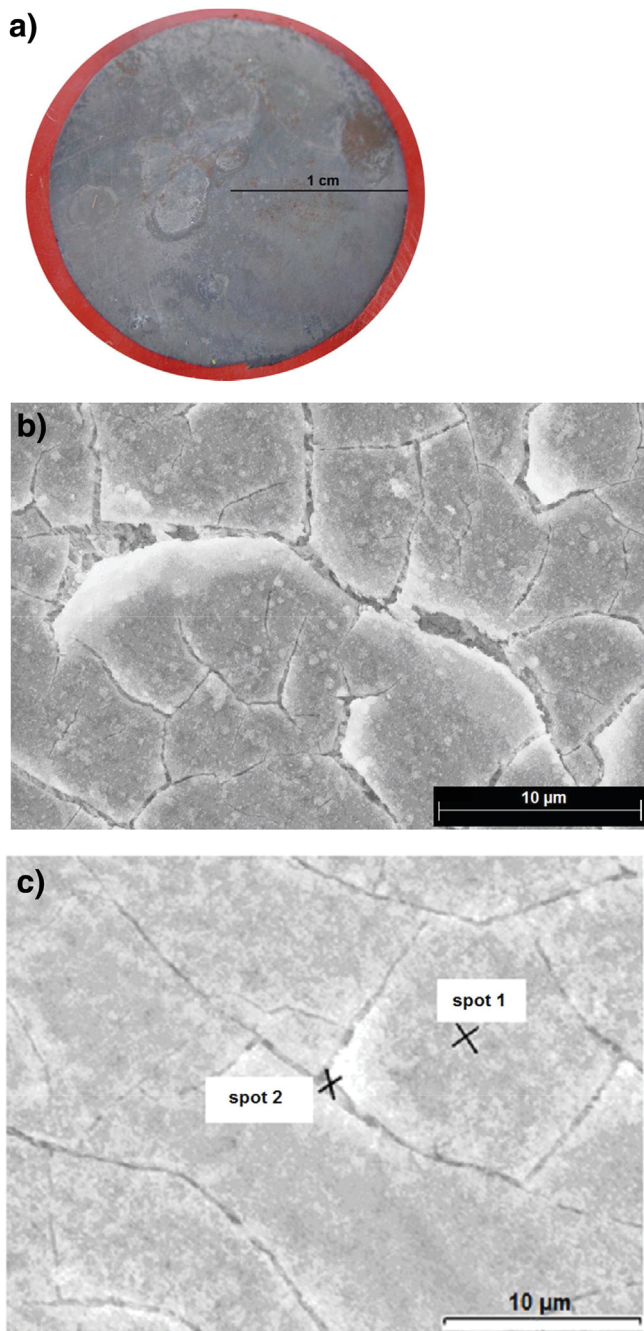


**Fig. 7.** Photograph (A) and SEM micrographs (B and C) of 1145 carbon steel surface after 24 hour immersion in anaerobic 10 mM phosphate solution pH 7.2 in the presence of 30  $\mu\text{L}$  heated hydrogenase. The markers in (C) indicate the positions where the EDX analyses were performed: on deposit (spot 1) and in a crack (spot 2). SEM characteristics: 10000  $\times$  magnification, 10 kV acceleration voltage.

especially because of its low solubility. It is indeed used by some industries as a corrosion protection method; the procedure is acid phosphating carried out at temperatures of up to 95  $^{\circ}\text{C}$  and at pH values between 2 and 3.5 with phosphates of zinc, iron or manganese, which leads to vivianite production [48]. Although the detailed mechanisms by which phosphate species lead to the formation of protective layers and the composition of the deposit obtained in phosphate solutions are still research topics, the main point is to have the right amount of Fe II (compared to Fe III) on the material surface that, in contact with the phosphate in the medium, leads to the formation of a vivianite deposit. This is the case in abiotic conditions when using chelating agent for instance [49]; the vivianite

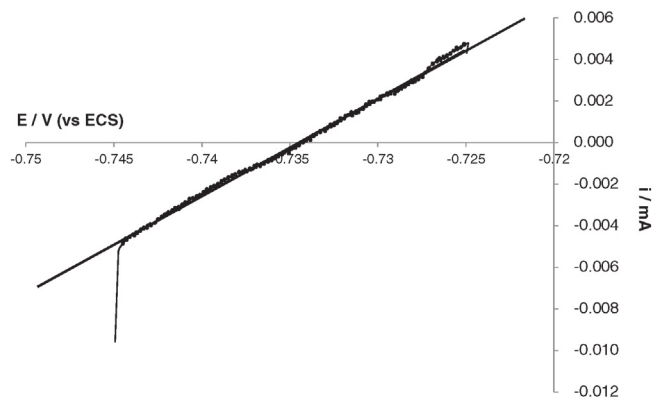


**Fig. 8.** Example of evaluation of  $R_p$  by plotting  $i = f(E)$  (potential scan rate: 0.2  $\text{mV s}^{-1}$ ) for 1145 carbon steel electrode during immersion in anaerobic 10 mM phosphate solution pH 7.2 in the presence of 30  $\mu\text{L}$  of hydrogenase. Regression equation:  $i \text{ (mA)} = 0.47(1/kW) \times E(V) + 0.35$  with  $R^2 = 0.9977$ .

layer deposit also depends on phosphate concentration [50,8], on how the preceding oxide layer forms, which is linked to the experimental conditions (electrode potential [51] and the presence or not of oxygen [47,52]). In biotic conditions, other mechanisms are suggested: oxygen consumption by the biofilm as the driving force to form vivianite [53], acceleration of Fe (III) reduction to Fe (II) in presence of microorganisms (such as *Geobacter sulfurreducens* [54]).

When hydrogenase was added into the solution, the fast variation of the open circuit potential with time, the visual and microscopic aspects of the coupon surfaces after 24 h, and the  $1/R_p$  values (reflecting  $i_{\text{corr}}$ ) confirmed a strong effect of hydrogenase on corrosion of carbon steel. It should be noted that the  $R_p$  measurements were done 4 h after hydrogenase injection, meaning when the open circuit potential had almost recovered a constant value (Figs. 1 and 5).  $R_p$  measurements were not performed before to avoid any disturbance during the first hours, period in which hydrogenase had the most obvious effect according to  $E_{\text{oc}}$  records. The different behaviours observed can consequently be attributed to the presence of hydrogenase only, without any parasite effect due to the measurements.  $1/R_p$  values recorded every 4 h were then almost constant (see Table 3), except when 80  $\mu\text{L}$  enzyme was added. Except in this latter case, the stability of  $1/R_p$  (thus  $i_{\text{corr}}$ ) and  $E_{\text{oc}}$  consistently indicated that the corrosion state reached 4 h after hydrogenase injection was roughly stable. Thus, the  $1/R_p$  values (as  $i_{\text{corr}}$ ) did not correspond to the period during which hydrogenase drastically affected the material, but they corresponded to the new surface steady state that was reached after hydrogenase injection.  $1/R_p$  values must consequently be commented not as direct measurements of the hydrogenase action, but as characteristics of the new state resulting from hydrogenase action.

The presence of hydrogenase always led to a fast increase in  $E_{\text{oc}}$ , the amplitude of which increased with the quantity of enzyme. Adding 30  $\mu\text{L}$  hydrogenase resulted in a visually more important deposit than in control experiments, with slight local pitting. It has already been claimed that hydrogenase can induce local cathodic sites that enhance iron dissolution in neighbouring anodic sites; the following precipitation of iron ions with phosphate forms a crystalline film partially composed of vivianite. Following this model, hydrogenase enhanced vivianite formation [32]. The observations made here are consistent with this mechanism. Adding 30  $\mu\text{L}$  hydrogenase favoured the formation of a better protective layer, as confirmed by the smaller  $1/R_p$  values ( $1.5 \cdot 10^{-4} \Omega^{-1} \text{cm}^{-2}$  instead of  $6.7 \cdot 10^{-4} \Omega^{-1} \text{cm}^{-2}$  in control experiments), representing smaller  $i_{\text{corr}}$ , that were recorded after 4 h. Larger amounts of hydrogenase (50 or 80  $\mu\text{L}$ ) resulted in visually more important deposits that contained more and more iron oxides/hydroxides. In these cases, iron dissolution and/or ion precipitation was enhanced to an extent that could no longer be balanced by the reaction with

**Table 3**  
Evolution of  $1/R_p$  versus time during the immersion of 1145 carbon steel coupons in anaerobic 10 mM phosphate solution pH 7.2, with or without hydrogenase;  $R_p$  is the polarisation resistance calculated through Stearn-Geary model.

Hydrogenase amount	$1/R_p$ ( $1/(\Omega \cdot \text{cm}^2)$ ) for t after injection						
	0 h	2 h	4 h	8 h	12 h	16 h	20 h
Control, no hydrogenase	<sup>a</sup> $7.6 \pm 2 \cdot 10^{-4}$	<sup>a</sup> $9.6 \pm 8 \cdot 10^{-4}$	<sup>b</sup> $6.7 \pm 1 \cdot 10^{-4}$	<sup>b</sup> $6.2 \pm 2 \cdot 10^{-4}$	<sup>b</sup> $5.9 \pm 1 \cdot 10^{-4}$	<sup>b</sup> $6.2 \pm 1 \cdot 10^{-4}$	<sup>b</sup> $6.6 \pm 1 \cdot 10^{-4}$
0 $\mu\text{L}$	–	–	$1.5 \cdot 10^{-4}$	$1.6 \cdot 10^{-4}$	$1.5 \cdot 10^{-4}$	$1.7 \cdot 10^{-4}$	$1.9 \cdot 10^{-4}$
30 $\mu\text{L}$	–	–	$4.0 \cdot 10^{-4}$	$3.4 \cdot 10^{-4}$	$2.9 \cdot 10^{-4}$	$3.1 \cdot 10^{-4}$	$3.3 \cdot 10^{-4}$
50 $\mu\text{L}$	–	–	$2.7 \cdot 10^{-4}$	$1.7 \cdot 10^{-4}$	$1.5 \cdot 10^{-4}$	$1.3 \cdot 10^{-4}$	$1.4 \cdot 10^{-4}$
80 $\mu\text{L}$	–	–	$2.4 \cdot 10^{-4}$	$2.2 \cdot 10^{-4}$	$2.0 \cdot 10^{-4}$	$1.9 \cdot 10^{-4}$	$1.8 \cdot 10^{-4}$
30 $\mu\text{L}$ -oxygenated	–	–	$1.3 \cdot 10^{-3}$	$8.7 \cdot 10^{-4}$	$4.0 \cdot 10^{-4}$	$3.1 \cdot 10^{-4}$	$2.6 \cdot 10^{-4}$
30 $\mu\text{L}$ -heated	–	–					

<sup>a</sup> Mean and standard deviation for 3 independent experiments.

<sup>b</sup> Mean and standard deviation for 7 independent experiments.

phosphate species, and corrosion products (oxides and hydroxides) accumulated in the layer.

In the presence of 30  $\mu\text{L}$  hydrogenase, the lower  $i_{\text{corr}}$  compared to control experiments can explain the higher value of  $E_{\text{oc}}$  obtained. Indeed it means that the anodic reaction decreased, and no supplementary hypothesis is required. With 50  $\mu\text{L}$  and 80  $\mu\text{L}$  hydrogenase,  $E_{\text{oc}}$  ennoblement was roughly proportional to the amount of hydrogenase, but  $i_{\text{corr}}$  kept similar values. It must be concluded that the catalysis of the cathodic process was also involved in  $E_{\text{oc}}$  increase. In the previous work that dealt with the effect of hydrogenase on vivianite formation [32], the cathodic reaction created by the presence of hydrogenase was due to the presence of phosphate and of a final electron acceptor (the natural redox partner of the enzyme). The cathodic reaction was consequently related to the Mechanism 1 described in the Introduction section. In contrast, the cathodic reaction detected here can only be the reduction of proton (or water) into hydrogen (Reaction (1)) catalysed by the hydrogenase because no other final reductant (electron acceptor) was present in solution.

Hydrogenase from *C. acetobutylicum* is highly sensitive to oxygen traces [55]. Keeping it at air, for more than 2 h, ensured complete loss of its catalytic properties for hydrogen oxidation. Adding hydrogenase after deactivating it in air led to an  $E_{\text{oc}}$  ennoblement similar to that with the same amount of active hydrogenase but, in contrast, the presence of the protein avoided the formation of any deposit and even protected the material surface against corrosion. Such behaviour was not linked to the phosphate medium. Similar observations were made in Tris-HCl pH 6.3: after 24 h, much of the surface remained mirror polished when 30  $\mu\text{L}$  deactivated hydrogenase was added, while control experiments in the absence of enzyme showed a homogeneous grey film (data not shown). In this case,  $E_{\text{oc}}$  ennoblement was due to the decrease of  $i_{\text{corr}}$  induced by the deactivated protein ( $1/R_p$  from  $6.7 \cdot 10^{-4}$  to  $2.4 \cdot 10^{-4} \Omega \cdot \text{cm}^{-2}$ ).  $E_{\text{oc}}$  ennoblement was not linked to a corrosion process but to some kind of protection of the material by the protein. Some complex links between “inert” proteins and the corrosion behaviour of metallic surfaces have already been reported in the literature. For instance, bovine serum albumin (BSA) adsorbed on iron-chromium alloy showed a protective effect against corrosion at pH 1.3, whereas it accelerated local corrosion at pH 5.5. In both cases, the protein has been assumed to affect the metal behaviour directly, as neither the thickness nor the composition of the protective layer was affected [56]. Using deactivated hydrogenase revealed that the simple protein shell, without enzymatic activity, have a remarkable protective effect. This effect due to the protein nature of hydrogenase was certainly also one of the causes of the  $i_{\text{corr}}$  decreases that were recorded with active hydrogenase. It must be concluded that hydrogenase affects the electrochemical behaviour of mild steel via different simultaneous effects. As already shown, adsorbed hydrogenase can catalyse the reduction of proton/water and induce local cathodic/anodic sites that enhance iron dissolution. In the presence of phosphate species this effect favours the formation of a protective layer containing vivianite [32]. This model remains consistent with the data obtained here. The protective effect of the

protein shell must now be added. Moreover large amounts of hydrogenase lead to the accumulation of iron oxides/hydroxides in the deposited layer, which gets a cracked structure.

Hydrogenase denatured by heating had the greatest effect on the electrochemical parameters and the deposit structure. An important deposit was observed with a heterogeneous, cracked structure. Obviously the corrosive effect of hydrogenase was not linked to its traditional activity for hydrogen oxido-reduction. Heating the enzyme completely denatured it, by unwinding and cutting the shell of amino acids that make up its structure. [Fe]-hydrogenases contain numerous Fe—S clusters that provide an electron transfer pathway between the buried active site and the molecular surface. [Fe]-hydrogenases have a domain with two [4Fe4S]-ferredoxin-like clusters not far from the active site, which are called mesial (FS4A) and distal (FS4B). In addition, the enzyme has a small domain containing a [4Fe—4S] cluster (called FS4C) and a plant-like ferredoxin domain with a [2Fe—2S] cluster (called FS2) [57,58]. Heating the enzyme resulted in its architecture exploding, exposing the metallic clusters to the external surroundings or even releasing the Fe—S clusters.

As an important conclusion to this work, it can be assumed that the catalysis of proton reduction was caused by the adsorption on the coupon surface of the iron-sulphur clusters contained in the hydrogenase. This hypothesis perfectly explains that corrosion enhancement was controlled by the amount of hydrogenase and that the effect was stronger after the enzyme had been denatured by heating. The catalysis of corrosion by hydrogenase may now be thought as another case of catalysis by iron-sulphur compounds. To some extent, the mechanisms suggested here may be compared with the mechanisms generally accepted for the microbial corrosion induced by sulphate reducing bacteria (SRB). SRB reduce sulphate to sulphide ions, which react with the iron ion forming iron sulphide FeS. FeS deposits catalyse proton reduction [16,17]. Cathodic zones (FeS) and anodic zones (Fe) are created on the same electrode, implying accelerated deterioration of the material by galvanic corrosion [59,60].

Hydrogenase from *C. acetobutylicum* contains 20 atoms of Fe (six in the active site, twelve in the [4Fe—4S]-type clusters (FS4A, FS4B, FS4C) and two in the [2Fe—2S]-type clusters (FS2) [39]). The concentration of hydrogenase in the initial aliquots was  $0.33 \times 10^{-6}$  M. When 30  $\mu\text{L}$  of the aliquot was injected into the 0.05 L electrochemical cell, the final concentration in the cell was  $2 \times 10^{-10}$  M. The overall amount of Fe contained in the electrochemical cell was then  $4 \times 10^{-9}$  M. In parallel, the hydrogenase has 18 atoms of sulphur (four in the H cluster, twelve in the [4Fe—4S] clusters: FS4A, FS4B, and FS4C and two in 2Fe2S: FS2). The total concentration of sulphur in the electrochemical cell was  $3.6 \times 10^{-9}$  M. These concentrations are very low, and it must be concluded that the specific iron clusters contained in the enzyme are highly efficient in catalysing proton reduction, certainly much more than the bulk iron sulphide deposits produced by SRB. Actually this conclusion is consistent with the function of these clusters inside the protein that contributes to the efficiency of

the reversible “proton reduction/hydrogen oxidation” reaction. Thanks to this redox chain, hydrogenase has an extremely high activity, of the order of 0.2 mol of hydrogen oxidised per minute per milligram of protein. Suitable adsorption of these clusters on the coupon surface should also be an important factor in efficiency. The presence of amino acids coming from the protein shell, even after unwinding or denaturing by heating, certainly promotes effective adsorption.

#### 4. Conclusion

Hydrogenase from *C. acetobutylicum* confirmed a high reactivity with surfaces of mild steel. Using less concentrated phosphate solution than in the previous work allowed a gradual effect of hydrogenase to be pointed out, which increased with its concentration in solution. These operating conditions also led to detect different effects of hydrogenase. The action of hydrogenase on mild steel surfaces must now be considered as the result of the complex combination of different elements: local catalysis of proton/water reduction that induces local iron dissolution, protective effect due to the protein shell, formation of a protective layer containing vivianite when phosphate species are present, cracked structure of the deposit that favours local corrosion. Moreover, the electrochemical action of hydrogenase is not only linked to its regular enzyme activity but also to the presence of the ion-sulphur compounds. The denatured enzyme revealed thus to be more active than the active hydrogenase.

Such a versatility of the phenomenon with respect to the experimental conditions, in particular the sensitivity of hydrogenase to oxygen, which makes it shift from an active enzyme to a protective protein, is certainly a main cause of the variety of results that have been reported in the literature so far on the possible role of hydrogenases in microbial corrosion. From this study, a pre-treatment based on the adsorption of inert proteins on steel surface could be proposed as an eco-friendly solution in the view to reduce the corrosion in field conditions. Moreover this work may also be a track to develop a new procedure for the deposit of vivianite protective layer on mild steel.

#### Acknowledgements

This work was supported by a grant from CNRS-DRI (BDI PED 2006). It was a part of CNRS European network “Surfaces of materials in living environments (SMILE)”.

The authors gratefully thank Luc Etcheverry (LGC) for his technical support, Marie-Line De Solan (LGC) for EDX facilities and Laurence Girbal and Marie Demuez (Laboratoire d'Ingénierie des Systèmes Biologiques et des procédés LISBP, INSA-Toulouse) for helpful discussions and for providing the hydrogenase aliquots.

#### References

- [1] I.B. Beech, Corrosion of technical materials in the presence of biofilms-current understanding and state-of-the art methods of study, *Int. Biodeterior. Biodegrad.* 53 (2004) 177–183.
- [2] W. Lee, Z. Lewandowski, P.H. Nielsen, W.A. Hamilton, Role of sulfate-reducing bacteria in corrosion of mild steel: a review, *Biofouling* 8 (1995) 165–194.
- [3] R. Javaherdashti, R.K. Singh Raman, C. Panter, E.V. Pereloma, Microbiologically assisted stress corrosion cracking of carbon steel in mixed and pure cultures of sulphate reducing bacteria, *Int. Biodeterior. Biodegrad.* 58 (2006) 27–35.
- [4] C. Xu, Y. Zhang, G. Cheng, W. Zhu, Pitting corrosion behavior of 316L stainless steel in the media of sulphate-reducing and iron-oxidizing bacteria, *Mater. Charact.* 59 (2008) 245–255.
- [5] C. Xu, Y. Zhang, G. Cheng, W. Zhu, Localized corrosion behavior of 316L stainless steel in the presence of sulfate-reducing and iron-oxidizing bacteria, *Mater. Sci. Eng.* 443 (2007) 235–241.
- [6] J. Duan, S. Wu, X. Zhang, G. Huang, M. Du, B. Hou, Corrosion of carbon steel influenced by anaerobic biofilm in natural seawater, *Electrochim. Acta* 54 (2008) 22–28.
- [7] R. Avci, B.H. Davis, M.L. Wolfenden, I.B. Beech, K. Lucas, D. Paul, Mechanism of MnS-mediated pit initiation and propagation in carbon steel in an anaerobic sulfidogenic media, *Corros. Sci.* 76 (2013) 267–274.
- [8] L. De Silva Muñoz, A. Bergel, R. Basséguy, Role of the reversible electrochemical deprotonation of phosphate species in anaerobic biocorrosion of steels, *Corros. Sci.* 49 (2007) 3988–4004.
- [9] W.P. Iverson, Mechanism of anaerobic corrosion of steel by sulfate reducing bacteria, *Mater. Perform.* 23 (1984) 28–30.
- [10] I.B. Beech, C.W.S. Cheung, Interactions of exopolymers produced by sulphate-reducing bacteria with metal ions, *Int. Biodeterior. Biodegrad.* 35 (1995) 59–72.
- [11] E. Miranda, M. Bethencourt, F.J. Botana, M.J. Cano, J.M. Sanchez-Amaya, A. Corzo, J.G. de Lomas, M.L. Fardeau, B. Ollivier, Biocorrosion of carbon steel alloys by an hydrogenotrophic sulfate-reducing bacterium *Desulfovibrio capillatus* isolated from a Mexican oil field separator, *Corros. Sci.* 48 (2006) (2417–243).
- [12] R. Javaherdashti, Impact of sulphate-reducing bacteria on the performance of engineering materials, *Appl. Microbiol. Biotechnol.* 91 (2011) 1507–1517.
- [13] Z.H. Dong, T. Liu, H.F. Liu, Influence of EPS isolated from thermophilic sulphate-reducing bacteria on carbon steel corrosion, *Biofouling* 27 (2011) 487–495.
- [14] D. Enning, J. Garrels, Corrosion of iron by sulfate-reducing bacteria: new views of an old problem, *Appl. Environ. Microbiol.* 80 (2014) 1226–1236.
- [15] H. Venzlaff, D. Enning, J. Srinivasan, K.J.J. Mayrhofer, A.W. Hassel, F. Widdel, et al., Accelerated cathodic reaction in microbial corrosion of iron due to direct electron uptake by sulfate-reducing bacteria, *Corros. Sci.* 66 (2013) 88–96.
- [16] R. Marchal, Involvement of sulfidogenic bacteria in iron corrosion, *Oil Gas Sci. Technol.* 54 (1999) 649–659.
- [17] W.A. Hamilton, Microbially influenced corrosion as a model system for the study of metal-microbe interactions: a unifying electron transfer hypothesis, *Biofouling* 19 (2003) 65–76.
- [18] K. Mori, H. Tsurumaru, S. Harayama, Iron corrosion activity of anaerobic hydrogen-consuming microorganisms isolated from oil facilities, *J. Biosci. Bioeng.* 110 (2010) 426–430.
- [19] R.D. Bryant, W.J. Jansen, J. Boivin, E.J. Laishley, W. Costerton, Effect of hydrogenase and mixed sulphate-reducing bacterial populations on the corrosion of steel, *Appl. Environ. Microbiol.* 57 (1991) 2804–2809.
- [20] C. Chatelus, P. Carrier, P. Saignes, M.F. Libert, Y. Berlier, P.A. Lespinat, et al., Hydrogenase activity in aged, nonviable *Desulfovibrio vulgaris* cultures and its significance in anaerobic biocorrosion, *Appl. Environ. Microbiol.* 53 (1987) 1708–1710.
- [21] A.V. Ramesh Kumar, R. Singh, R.K. Nigam, A.V.R. Kumar, R. Singh, R.K. Nigam, Mossbauer spectroscopy of corrosion products of mild steel due to microbiologically influenced corrosion, *J. Radioanal. Nucl. Chem.* 242 (1999) 131–137.
- [22] D.J. Evans, C.J. Pickett, Chemistry and the hydrogenases, *Chem. Soc. Rev.* 32 (2003) 268–275.
- [23] F.A. Armstrong, Hydrogenases: active site puzzles and progress, *Curr. Opin. Chem. Biol.* 8 (2004) 133–140.
- [24] R. Mertens, A. Liese, Biotechnological applications of hydrogenases, *Curr. Opin. Biotechnol.* 15 (2004) 343–348.
- [25] A. Pardo, A.L. De Lacey, V.M. Fernandez, H.J. Fan, Y. Fan, M.B. Hall, Density functional study of the catalytic cycle of nickel-ion [NiFe] hydrogenase and the involvement of high-spin nickel(II), *J. Biol. Inorg. Chem.* 11 (2006) 286–306.
- [26] E.J. Lyon, S. Shima, G. Buurman, S. Chowdhuri, A. Batschauer, K. Steinbach, R.K. Thauer, UV-A/blue-light inactivation of “the metal-free” hydrogenase (Hmd) from methanogenic archaea, *Eur. J. Biochem.* 271 (2004) 195–204.
- [27] M. Frey, Hydrogenases: hydrogen-activating enzymes, *Chem. Biochem.* 3 (2002) 153–160.
- [28] M.D. Yates, M. Siegert, B.E. Logan, Hydrogen evolution catalyzed by viable and non-viable cells on biocathodes, *Int. J. Hydrog. Energy* 39 (2014) 16841–16851.
- [29] R.D. Bryant, E.J. Laishley, The role of hydrogenase in anaerobic corrosion, *Can. J. Microbiol.* 36 (1990) 259–264.
- [30] R.D. Bryant, E.J. Laishley, The effect of inorganic phosphate and hydrogenase on the corrosion of mild steel, *Environ. Biotechnol.* 38 (1993) 824–827.
- [31] S. DaSilva, R. Basseguy, A. Bergel, Electrochemical deprotonation of phosphate on stainless steel, *Electrochim. Acta* 49 (2004) 4553–4561.
- [32] S. DaSilva, A. Bergel, R. Basseguy, Hydrogenase-catalysed deposition of vivianite on mild steel, *Electrochim. Acta* 49 (2004) 2097–2103.
- [33] O.A. Zadovny, N.A. Zorin, I.N. Gogotov, Transformation of metals and metal ions by hydrogenases from phototrophic bacteria, *Arch. Microbiol.* 84 (2006) 279–285.
- [34] A. Nedoluzhko, I.A. Shumilin, L.E. Mazhorova, V.O. Popov, V.V. Nikandrov, Enzymatic oxidation of cadmium and lead metals photodeposited on cadmium sulphide, *Bioelectrochem* 53 (2001) 61–71.
- [35] J.S. Deutzmann, M. Sahin, A.M. Spormann, Extracellular enzymes facilitate electron uptake in biocorrosion and bioelectrosynthesis, *MBio.* 6 (2015), e00496 (–15–).
- [36] M.J. Lukey, A. Parkin, M.M. Roessler, B.J. Murphy, J. Harmer, T. Palmer, et al., How *Escherichia coli* is equipped to oxidize hydrogen under different redox conditions, *J. Biol. Chem.* 285 (2010) 3928–3938, <http://dx.doi.org/10.1074/jbc.M109.067751>.
- [37] S. Da Silva, R. Basséguy, A. Bergel, Electron transfer between hydrogenase and 316L stainless steel: identification of a hydrogenase-catalyzed cathodic reaction in anaerobic mic, *J. Electroanal. Chem.* 561 (2004) 93–102.
- [38] M. Mehanna, R. Basséguy, M.L. Délia, L. Girbal, M. Demuez, A. Bergel, New hypotheses for hydrogenase implication in the corrosion of mild steel, *Electrochim. Acta* 54 (2008) 140–147.
- [39] L. Girbal, G. Von Abendroth, M. Winkler, P.M.C. Benton, I. Meynial-Salles, C. Croux, J.W. Peters, T. Happe, P. Soucaille, Homologous and heterologous overexpression in *Clostridium acetobutylicum* and characterization of purified Clostridial and algal Fe-only hydrogenases with high specific activities, *Appl. Environ. Microbiol.* 71 (2005) 2777–2781.
- [40] B. Elsener, Corrosion rate of steel in concrete-measurements beyond the Tafel law, *Corros. Sci.* 47 (2005) 3019–3033.
- [41] M. Stern, A.L. Geary, Electrochemical polarization, *J. Electrochem. Soc.* 104 (1) (Jan. 1957) 56.
- [42] G. McGowan, J. Prangnell, The significance of vivianite in archaeological settings, *Geoarchaeology* 21 (2006) 93–111.

- [43] D. Glindemann, F. Eismann, A. Bergmann, P. Kusch, U. Stottmeister, Phosphine by bio-corrosion of phosphide-rich iron, *Environ. Sci. Pollut. Res.* 5 (1998) 71–74.
- [44] W.P. Iverson, G.J. Olson, Technical Summary Report No. 1, National Bureau of Standards, National Measurement Lab., Washington DC, 1982.
- [45] J.J. Robin, J. Duran, L. Cot, A. Bonnel, M. Duprat, F. Dabosi, Physicochemical and electrochemical study of the protection of a carbon-steel by monofluorophosphates. 1. Influence of a chemical conversion treatment, *Appl. Electrochem.* 12 (1982) 701–710.
- [46] Techniques de l'ingénieur, Corrosion des aciers au carbone section 3.2.1.
- [47] E.M.A. Martini, S.T. Amaral, I.L. Müller, Electrochemical behaviour of invar in phosphate solutions at pH = 6, *Corros. Sci.* 46 (2004) (2907–2115).
- [48] W. Rausch, Die Phosphatierung Von Metallen, Leuze Verlag, Saulgau, Germany. The Phosphating of Metals English Electronic Version 1990, 1988.
- [49] H. Harms, H.-P. Volkland, G. Repphun, A. Hiltolt, O. Wanner, A.J.B. Zehnder, Action of chelators on solid iron in phosphate-containing aqueous solutions, *Corros. Sci.* 45 (2003) 1717–1732.
- [50] Y. Gourbeyre, E. Guilminot, F. Dalard, Study of the corrosion layer on iron obtained in solutions of water-polyethylene glycol (PEG400)-sodium phosphate, *J. Mater. Sci.* 38 (2003) 1307–1313.
- [51] C.A. Borrás, R. Romagnoli, R.O. Lezna, In-situ spectroelectrochemistry (UV-visible and infrared) of anodic films on iron in neutral phosphate solutions, *Electrochim. Acta* 45 (2000) 1717–1725.
- [52] A. Paszternák, I. Felhósi, Z. Pászti, E. Kuzmann, A. Vértes, E. Kálmán, L. Nyikos, Surface analytical characterization of passive iron surface modified by alkyl-phosphonic acid layers, *Electrochim. Acta* 55 (2010) 804–812.
- [53] H.-P. Volkland, H. Harms, B. Müller, G. Repphun, O. Wanner, A.J.B. Zehnder, Bacterial phosphating of mild (unalloyed) steel, *Appl. Environ. Microbiol.* 66 (2000) 4389–4395.
- [54] C. Cote, O. Rosas, R. Basséguy, *Geobacter sulfurreducens*: an iron reducing bacterium that can protect carbon steel against corrosion? *Corros. Sci.* 94 (2015) 104–113.
- [55] M. Demuez, L. Cournac, O. Guerrini, P. Soucaille, L. Girbal, Complete activity of *Clostridium acetobutylicum* [FeFe]-hydrogenase and kinetic parameters for endogeneous redox partners, *FEMS Microbiol. Lett.* 275 (2007) 113–121.
- [56] I. Frateur, L. Lartundo-Rojas, C. Méthivier, A. Galtayries, P. Marcus, Influence of bovine serum albumin in sulphuric acid aqueous solution on the corrosion and the passivation of an iron-chromium alloy, *Electrochim. Acta* 51 (2006) 1550–1557.
- [57] J.C. Fontecilla-Camps, A. Volbeda, C. Cavazza, Y. Nicolet, Structure/function relationships of [NiFe] and [FeFe]-hydrogenases, *Chem. Rev.* 107 (2007) 4273–4303.
- [58] J.W. Peters, W.N. Lanzilotta, B.J. Lenon, L.C. Seefeldt, X-ray crystal structure of the Fe-only hydrogenase (Cpl) from *Clostridium pasteurianum* to 1.8 angstrom resolution, *Science* 282 (1998) 1853–1858.
- [59] I. Dupont-Morral, Les bactéries sulfato-réductrices et la corrosion bactérienne, *Bull. Soc. Fr. Microbiol.* 19 (2004) 108–115.
- [60] R.A. King, J.D.A. Miller, Corrosion of mild steels by iron sulphides, *Br. Corros.* 8 (1973) 137–141.